Title

Multi-Imaging Method to Assay the Contractile Mechanical Output of Micropatterned Human iPSC-Derived Cardiac Myocytes.

Journal

Circulation Research, 120(10)

Authors

Ribeiro, Alexandre
Schwab, Olivier
Mandegar, Mohammad
et al.

Publication Date

2017-05-12

DOI

10.1161/CIRCRESAHA.116.310363

Peer reviewed

Published in final edited form as:

Circ Res. 2017 May 12; 120(10): 1572–1583. doi:10.1161/CIRCRESAHA.116.310363.

Multi-Imaging Method to Assay the Contractile Mechanical Output of Micropatterned Human iPSC-Derived Cardiac Myocytes

Alexandre J. S. Ribeiro[1,4,5], **Olivier Schwab**[1], **Mohammad A. Mandegar**[5], **Yen-Sin Ang**[5,6], **Bruce R. Conklin**[5,8,9,10], **Deepak Srivastava**[5,6,7], and **Beth L. Pruitt**[1,2,3,4]

[1]Department of Mechanical Engineering, Stanford University, Stanford, CA 94305, USA

[2]Department of Molecular and Cellular Physiology (by courtesy), Stanford University, Stanford, CA 94304, USA

[3]Department of Bioengineering (by courtesy), Stanford University, Stanford, CA 94305, USA

[4]Stanford Cardiovascular Institute, Stanford University, Stanford, CA 94309, USA

[5]Gladstone Institute of Cardiovascular Disease, San Francisco, CA 94158, USA

[6]Roddenberry Stem Cell Center at Gladstone, San Francisco, CA 94158, USA

[7]Departments of Pediatrics and Biochemistry & Biophysics, University of California, San Francisco, San Francisco, CA 94158, USA

[8]Department of Cellular and Molecular Pharmacology, University of California, San Francisco, San Francisco, CA 94158, USA

[9]California Institute for Quantitative Biosciences, QB3, University of California, San Francisco, San Francisco, CA 94158, USA

[10]Department of Medicine and Cellular and Molecular Pharmacology, University of California, San Francisco, San Francisco, CA 94158, USA

Abstract

Rationale—During each beat, cardiac myocytes generate the mechanical output necessary for heart function through contractile mechanisms that involve shortening of sarcomeres along myofibrils. Human induced pluripotent stem cells can be differentiated into cardiac myocytes that model cardiac contractile mechanical output more robustly when micropatterned into physiological shapes. Quantifying the mechanical output of these cells enables us to assay cardiac activity in a dish.

Objective—We sought to develop a computational platform that integrates analytical approaches to quantify the mechanical output of single micropatterned cardiac myocytes from microscopy videos.

Address correspondence to: Dr. Beth Pruitt, 452 Escondido Mall, Building 520, Room 228, Stanford, CA 94305-4040, Phone: +1.650.723.4133, Fax: +1.650.725.1587, pruitt@stanford.edu.

DISCLOSURES

None.

Methods and Results—We micropatterned single cardiac myocytes differentiated from human induced pluripotent stem cells on deformable polyacrylamide substrates containing fluorescent microbeads. We acquired videos of single beating cells, of microbead displacement during contractions, and of fluorescently labeled myofibrils. These videos were independently analyzed to obtain parameters that capture the mechanical output of the imaged single cells. We also developed novel methods to quantify sarcomere length from videos of moving myofibrils and to analyze loss of synchronicity of beating in cells with contractile defects. We tested this computational platform by detecting variations in mechanical output induced by drugs and in cells expressing low levels of myosin binding protein C.

Conclusions—Our method can measure cardiac function in cardiac myocytes differentiated from induced pluripotent stem cells and determine contractile parameters that can be used to elucidate the mechanisms that underlie variations in cardiac myocyte function. This platform will be amenable to future studies of the effects of mutations and drugs on cardiac function.

Keywords

Cardiac myocyte; contractility; stem cell; single cell; sarcomere length

Subject Terms

Contractile Function; Myocardial Biology

INTRODUCTION

Cardiac myocytes (CMs) are the muscle cells of the myocardium that beat to generate the mechanical output required for heart function.[1] The mechanical output of CMs originates from the shortening of sarcomeres aligned in series along myofibrils.[2] Human induced pluripotent stem cells (hiPSCs) can be differentiated into beating CMs (hiPSC-CMs).[3]

However, myofibrils in hiPSC-CMs are disorganized and not aligned as myofibrils in primary CMs;[4] this disarray has been a limiting factor in applying hiPSC-CMs for assaying cardiac function in vitro.[4] Micropatterning of hiPSC-CMs on substrates can successfully induce intracellular alignment of myofibrils,[5] thereby enhancing the maturity of their contractile machinery and positioning these engineered cells as models of cardiac contractility.[6–10] By micropatterning hiPSC-CMs on compliant substrates with known mechanical properties, their mechanical output can be calculated through non-destructive and minimally invasive microscopy-based approaches (Figure 1A).[6–8] Other approaches also include tracking cell movement from videos of beating cells acquired with bright-field microscopy[8, 11–13] and using deformable microposts as substrates that measure cell forces.[14] Mechanical output has also been assayed with engineered multicellular systems composed of hiPSC-CMs or co-cultured with other cell types.[15] Induced intracellular alignment of myofibrils is central for accelerating the contractile maturity of hiPSC-CMs.[16] Myofibrils are easier to image in single cell systems, allowing the assessment of these structures in live hiPSC-CMs.[7]

There has been a considerable increase in the use of single micropatterned hiPSC-CMs to model cardiac contractile activity in vitro with a variety of video-based methods.[6–10] These methods include: 1) quantifying the contractile movement of hiPSC-CMs imaged with bright-field, 2) measuring the displacement of myofibrils and measuring the varying length of sarcomeres, and/or 3) estimating cell-generated tractions using traction force microscopy. However, the field of hiPSC-CM contractile assessment lacks an integrated platform that enables these distinct properties to be measured simultaneously and coherently.

Here, we present a computational platform that integrates distinct image-based methods to analyze mechanical output from videos of micropatterned hiPSC-CMs on deformable polyacrylamide substrates (Figure 1). Our platform analyzes bright-field videos of single cells, videos of the substrate moving due to cell-generated tractions, and videos of labeled myofibrils (Online Figure I). These analyses yield a set of parameters that characterize the mechanical output of hiPSC-CMs. We also present novel approaches to measure sarcomere length from videos of moving myofibrils and to quantify the loss of synchronicity of contractile movement within a single cell due to contractile defects. Our analytical platform detected drug-induced effects on the mechanical output of micropatterned hiPSC-CMs, as well as contractile defects due to decreased expression of the gene that encodes myosin binding protein C3 (MYBPC3), thus validating its ability to assay cardiac contractility under pharmacological conditions or in modeling cardiac disease. We made this tool easily accessible to enable future research using hiPSC-CMs[17–19] with higher throughput and reduced user effort.

METHODS

Detailed methods are provided in the Online Supplemental Material. We acquired videos of single micropatterned hiPSC-CMs cultured on polyacrylamide hydrogels (Online Figure II) to analyze the mechanical output of their contractile cycles (Figure 1A). We acquired three types of videos via microscopy: bright-field videos (Online Movie I), videos of fluorescent microbeads in the substrate (Online Movie II), and videos of fluorescent myofibrils (Online Movie III). Each video showed movements of the substrate, cell surface, and myofibrils (Figure 1A). For each video frame, we quantified the average displacement (d) of the imaged moving structures (cells, microbeads and myofibrils) and the velocity (V) of this movement. Contractile forces were estimated after submitting the videos of substrate displacement to traction force microscopy[7] and we calculated the magnitude of force vectors (F) from traction stresses (Online Movie II). Sum of F (ΣF) was estimated and we multiplied ΣF by V to calculate power (P). We determined parameters from the plotted curves of these properties (d, V, ΣF, and P; Figure 1; Online Figures I and III). We calculated d with time (d-curves) and V with time (V-curves) (Figure 1B–L) with the cross-correlation algorithm Ncorr[20] (Figure 1). For a region of interest (ROI) defined by the cell borders (Figure 1B), we calculated d (Figure 1C) and V (Figure 1D). We also determined the movement of microbeads (Figure 1D) within a region of the substrate surface delimited by an ellipse of dimensions that are proportional to the area of the ROI, yielding d-curves (Figure 1F) and V-curves (Figure 1G) of the microbeads. For each video frame, we estimated ΣF, yielding F-curves (Figure 1H). We plotted P with time (P-curves) (Figure 1I) and also quantified myofibril movement (Figure 1J) to determine d-curves (Figure 1K) and V-curves (Figure

1L). The beat rate (*br*) of cells was derived from *d*-curves. Peak displacement (d_{max}) and peak force (ΣF_{max}) were obtained from the peaks of *d*-curves and *F*-curves, respectively (Online Figure III). From *V*-curves (Online Figure III), we determined the peak velocity of contraction (V_C) and the peak velocity of relaxation (V_R). Peak power of contraction (P_C) and peak power of relaxation (P_R) were derived from *P*-curves (Online Figure III). We also calculated a time parameter ($\hat{t}$) representing the time between contraction and relaxation peaks (Figure 2). We quantified sarcomere length in videos of myofibrils in micropatterned hiPSC-CMs (Online Figure IV).

RESULTS

Contractile and kinetic parameters derived from image-based analysis robustly describe cell mechanical output

The properties plotted in Figure 1 were the basis for deriving quantitative parameters that were used to analyze the contractile mechanical output of single micropatterned hiPSC-CMs. However, calculating the data in Figure 1 relied on the cross-correlation algorithm Ncorr to systematically analyze movement with high precision.

To determine whether Ncorr was suitable for quantifying contractile displacement, we compared it with two other cross-correlation algorithms that have been used to analyze movement at the micron scale: PIVlab[21] and ImageJ PIV (Online Figure V).[22] When we processed the ROI defined by the cell borders in Online Movie IV with Ncorr, PIVlab, and ImageJ PIV, we obtained similar *d*-curves (Online Figure V). We then decreased the image resolution and added noise to the frames of Online Movie IV to test whether the cross-correlation approaches yielded similar results independently of the video quality. Ncorr performed better in systematically yielding the same displacements from videos with varying image quality. Ncorr provided more consistent results for performing all the analyses in Figure 1.

Overall, we calculated two classes of parameters to describe the mechanical output of micropatterned hiPSC-CMs: contractile parameters and kinetic parameters. Contractile parameters, such as d_{max} and ΣF_{max} (Online Figure III), relate to the maximal amount of total stress that each cell generates on the surface during its contractile cycle. V_C, V_R, and *br* are kinetic parameters (Online Figure III). We also calculated the kinetic parameter $\hat{t}$ (Figure 2A), which scales with the total time of contraction and can also be simply determined from *V*-curves. For example, we observed an increase in $\hat{t}$ after exposing the cell to low doses of caffeine by slowly diffusing it through the cell-culture medium (Figure 2B). This observation clearly illustrated how $\hat{t}$ scales with the time of each contractile cycle. In addition, we included the calculation of P_C and P_R in our analytical platform because these provide both contractile and kinetic information (Online Figure I), since *P* is calculated from ΣF and *V*.

We added caffeine to the extracellular milieu of a single hiPSC-CM (Figure 2B and C) and recorded videos of moving microbeads in the substrate in order to validate the ability of the described parameters to quantify contractile variations. In addition to an increase in $\hat{t}$, we also detected variations in d_{max}, br, P_C, and P_R upon adding caffeine to the extracellular

milieu (Figure 2B and C). This observation suggested that our approach is suitable for detecting the effects of drugs that alter contractile activity.

Parameters from image-based analysis can quantify drug-induced contractile variations

Specific drugs change the contractile activity of hiPSC-CMs by affecting pathways or proteins that regulate CM function.[23] We tested the ability of our platform to detect variations in mechanical output induced by isoproterenol and omecamtiv mecarbil.

Isoproterenol—Isoproterenol is a positive inotrope, which corresponds to increases in mechanical output and increase in *br*, respectively. Isoproterenol activates the β-adrenergic pathway and affects the contractility of CMs in a dose-dependent manner.[24] We aimed to validate the ability to detect different effects of different drug concentrations with isoproterenol and we observed different contractile responses to 0.1 and 1 μM in micropatterned hiPSC-CMs (Figure 3 and Online Figure VI). For the same single cell, we estimated ΣF with traction force microscopy (Figure 3A–C), determined the movement of fluorescently labeled myofibrils (Figure 3D–F), and the movement of the cell imaged with bright-field microscopy (Figure 3G–I). Both ΣF_{max} and *br* increased when 0.1 μM isoproterenol was added to the medium (Figure 3B), as did P_C and P_R (Figure 3C). 1 μM isoproterenol induced a substantial decrease in all parameters, except for a clear increase in *br* (Figure 3 and Online Table 1). Curves obtained from processing videos of moving fluorescent myofibrils (Figures 3E and 3F, Online Movies V, VI, and VII) and bright-field videos of moving cells (Figures 3H and 3I) showed similar trends. Variations in *d*-curves and *V*-curves were consistent with those obtained from *F*-curves and *P*-curves (Figure 3). In these analyses, d was a proxy for ΣF and *V* was a proxy for *P*. Increases in d_{max}, *br*, V_C, and V_R were detected when isoproterenol was added at 0.1 μM (Figure 3 and Online Table 1). As observed from traction force microscopy analysis (Figure 3A–C), also with myofibril and cell movements, a more pronounced increase in *br* occurred after adding 1 μM isoproterenol, but the absolute values of d_{max}, V_C, and V_R decreased (Figure 3 and Online Table 1).

Next, to validate the consistency of our approach, we used traction force microscopy (Online Figure VI) and cross-correlation of brighfield videos (Online Figure VI) to measure contractile variations in 6 more single micropatterned hiPSC-CMs incubated first in 0.1 μM and then in 1 μM isoproterenol (Online Figure VI). We aimed to test if the detected effects of isoproterenol were consistent between different single cells and if results from traction force microscopy matched results of cross-correlation of bright-field videos. Overall from *F*-curves, we observed increases in ΣF_{max} and *br* at 0.1 μM isoproterenol, followed by a more pronounced increase in *br* and a decrease in ΣF_{max} for 1 μM isoproterenol (Online Figure VI A–C). We calculated parameters of mechanical output from traction force microscopy analysis to test consistency of variations among different cells and further validated this platform for use in these types of studies (Online Figure VI D–K). Traction force microscopy revealed variations in the following parameters that differed between 0.1 and 1 μM isoproterenol: d_{max}, V_C, V_R, ΣF_{max}, P_C, and P_R (Online Figure VI D–F and I–K). The absolute values of these parameters for each cell consistently increased for 0.1 μM isoproterenol and decreased for 1 μM isoproterenol (Online Figure VI). Values of $\hat{t}$ decreased (Online Figure VI G), and values of *br* increased (Online Figure VI H) for either

concentration of isoproterenol. These results demonstrated the ability of our traction force microscopy-based analytical tool to detect effects of different drug concentrations in the mechanical output of populations of micropatterned hiPSC-CMs.

We next tested whether parameters derived from quantifying cellular movement on bright-field videos (Online Figure VI L–O) showed the same levels of variation observed from traction force microscopy. We generally detected similar trends in variations of parameters (d_{max}, V_C, V_R, $\hat{t}$) calculated from the analysis of displacements within ROIs in bright-field videos of cells incubated in different concentrations of isoproterenol. However, the differences in variations of parameters detected with traction force microscopy for each concentration of isoproterenol were statistically significant, while no statistical significance was observed between differences in variations of bright-field cell displacement parameters. Even if the trend is similar between results from traction force microscopy and results from bright-field analysis, this observation suggests that results extracted from traction force microscopy may detect these differences more robustly. In addition, the variations in ΣF_{max}, P_C, and P_R measured with traction force microscopy (Figures 3B and 3C) after adding isoproterenol were more pronounced than the variations in d_{max}, V_C, and V_R measured from the video of moving myofibrils (Figures 3E and 3F) or from the bright-field video of a beating cell (Figures 3H and 3I).

Omecamtiv mecarbil

We incubated cells in omecamtiv mecarbil, which directly affects cardiac-specific myosin-actin interactions by accelerating the transition of myosin binding to actin toward a strongly bound state.[25] We tested the effects of 0.1 μM and 10 nM omecamtiv mecarbil on the mechanical output of micropatterned hiPSC-CMs and calculated variations in parameters derived from traction force microscopy (Online Figure VII A–H). We used different cell populations (n=6) for each concentration values. We first acquired videos within 5 min of adding omecamtiv mecarbil to the culture medium. Variations in $\hat{t}$ and br were statistically different between cells incubated in 0.1 μM and 10 nM omecamtiv mecarbil (Online Figure VII D and E). In short, we observed decreased mechanical output (negative inotropy) of micropatterned hiPSC-CMs induced by omecamtiv mecarbil and chronotropic effects depended on the drug dose (Online Figure VII I).

We then tested the acute effects of omecamtiv mecarbil on the mechanical output of a single cell within the initial seconds of incubation (Online Figure VII J). In contrast to chronic effects minutes after drug addition, we observed positive inotropy within 10 s of adding 0.1 μM omecamtiv mecarbil (Online Figure VII J). We further tested the ability of our platform to investigate these differences in acute and chronic effects in one single micropatterned hiPSC-CM with labeled myofibrils (Figure 4A and Online Movie VII). For this cell, we acquired videos of microbeads (for traction force microscopy), of myofibrils and of the cell and calculated contractile parameters from these data. We observed distinct differences in sarcomere activity between acute (Figure 4B and Online Movie IX) and chronic (Figure 4C and Online Movie X) responses to omecamtiv mecarbil. The acute response of this single hiPSC-CM to omecamtiv mecarbil involved changes in sarcomere organization (Figure 4B) and movement (Online Movie IX). For each contractile cycle, we observed oscillatory

contractions of sarcomeres and overlap between sarcomeres (Online Movie IX). Chronic myofibril damage was evident for this cell, but also when other hiPSC-CMs were incubated in 1 μM and 10 nM omecamtiv mecarbil (Online Figure VIII). These results demonstrated the value of our analytical approach for being able to simultaneously measure acute and chronic effects of the same drug.

We also asked whether parameters obtained from traction force microscopy (Figures 4D and 4E) could be related to parameters obtained from analyzing moving myofibrils (Figures 4F and 4G) and cell movement imaged with bright-field (Figure 4H and 4I). As also shown in Online Figure VI J, we observed slight acute increases in ΣF_{max} and br for the tested cell (Figure 4D). However, the absolute values of P_C and P_R did not seem to considerably vary after adding omecamtiv mecarbil (Figure 4E). Analysis of myofibril movement yielded similar variations in parameters of mechanical output: the acute values of d_{max} and br slightly increased (Figure 4F), but no considerable acute variations were observed in V_C and V_R (Figure 4G). In contrast to our experiment with isoproterenol (Figure 4), cell-movement analysis yielded results that differed from the results of analysis of movement of myofibrils when cells were exposed to omecamtiv mecarbil. Bright-field videos indicated a considerable acute increase in d_{max} (Figure 4H) and increases in the absolute values of V_C and V_R (Figure 4I, Online Table I).

Overall, for tested variations in mechanical output induced by omecamtiv mecarbil, data based on traction force microscopy and myofibril movement seemed to coincide, but differed from data based on changes in cell movement on bright-field microscopy. Parameters are presented in Online Table I for the cell exposed to both concentrations of isoproterenol (Figure 3) and the cell analyzed after acute and chronic exposure of omecamtiv mecarbil (Figure 4), demonstrating our platform's potential for quantifying the contractile effects of drugs.

Variations in sarcomere length relate to changes in mechanical output

Labeling live myofibrils allows for the quantification of sarcomere length during a contractile cycle.[7] We developed an automated tool to quantify sarcomere length for each frame of a video of micropatterned hiPSC-CMs with labeled myofibrils (Online Figure IV). We also validated the ability to measure variations in sarcomere length induced by isoproterenol and omecamtiv mercanbil. For this purpose, we used the myofibril videos of the cell presented in Figure 3 (Online Movies V, VI, and VII) and of the cell presented in Figure 4 (Online Movies VIII, IX and X). For the method developed for calculating sarcomere length, we skeletonized sarcomeres for each frame (Online Movie XI and Online Movie XII), obtained heat maps of sarcomere length within single micropatterned hiPSC-CMs for each frame (Online Movie XIII), and calculated sarcomere shortening by subtracting the minimal values of average sarcomere length from the maximal values of sarcomere length (Online Figure IX). We then analyzed average sarcomere length (Figure 5) for the cell exposed to isoproterenol (Figure 3 and Online Movies V–VII) and for the cell for which acute and chronic effects of omecamtiv mecarbil were captured in video (Figure 4 and Online Movies VIII–X). We calculated average sarcomere length values for all frames of the

videos, as well as maximal sarcomere length, minimal sarcomere length, and sarcomere shortening (Figure 5).

We aimed to test whether detected variations in mechanical output (Figures 3, 4 and Online Figures VI and VII) could relate to sarcomere length and sarcomere shortening, as well as whether measurements of sarcomere properties yield information on drug-induced changes in CM function. Both isoproterenol (Figure 5A–D) and omecamtiv mecarbil (Figure 5E–H) decreased average values of sarcomere length, but had different effects on sarcomere shortening. The isoproterenol-induced decrease in sarcomere length was accentuated at 1 μM (Figure 5A); at this concentration, the maximal mean values of sarcomere length also decreased relative to the level before the addition of isoproterenol (Figure 5B). Minimal average sarcomere length values decreased with 0.1 μM of isoproterenol and decreased even more at 1 μM (Figure 5A). In addition, sarcomere shortening considerably increased with 0.1 μM isoproterenol (Figure 5D), which may be related to the increase in mechanical output evident at this concentration (Figure 3). Chronic and acute effects of omecamtiv mecarbil also induced decreases in average sarcomere length (Figure 5E), maximal average sarcomere length (Figure 5F), and minimal average sarcomere length (Figure 5G). No omecamtiv mecarbil-induced variations were detected in sarcomere shortening (Figure 5H). Taken together, these data validate our method for measuring sarcomere length within micropatterned hiPSC-CMs.

Intracellular asynchronicity of movement predicts defective contractility

The intracellular space of mature primary CMs beats synchronously during each contractile cycle.[26–29] Loss of synchronicity in muscular contractions is a marker of loss of myocardial function, which can originate from extracellular or intracellular disorders that lead to heart failure.[30, 31] Pathologic myocardial disarray is intimately related to asynchronicity of beating and loss of myofibril organization.[32, 33] To test the hypothesis that asynchronicity of hiPSC-CM beating could serve as an assay of disease state, we defined two parameters of asynchronicity (see Online Methods): spatial asynchronicity (a_θ) versus temporal asynchronicity (a_δ) of contractile movement. a_θ was calculated from the direction of movement of all pixels that differed from the average direction of movement. a_δ was calculated from the offset times (Figure 6A) of each pixel within a ROI (Figure 6B) and provides information about when movement occurs within the cell relative to the average timing of contraction (Figure 6C). We measured the parameters a_θ and a_δ to detect potential contractile defects in hiPSC-CMs with reduced expression of MYBPC3, which has been associated with pathological cardiac hypertrophy in mice due to disarray of the myocardium at the cellular and myofibril levels.[34, 35] We consistently observed increases in a_θ (Figure 6D) and a_δ (Figure 6E) in hiPSC-CMs with decreased expression of MYBPC3 (Online Figure X). In addition, these cells had decreased values of $\hat{t}$ (Figure 6F) and ΣF_{max} (Figure 6G), as previously reported.[9] These results demonstrate that contractile defects can be detected by analyzing the asynchronicity of movement in micropatterned hiPSC-CMs.

DISCUSSION

Here, we present an integrated approach for analyzing the mechanical output of micropatterned hiPSC-CMs from videos acquired via live-cell imaging (Figure 1). We extracted parameters that characterized the mechanical performance of hiPSC-CMs as well as information about sarcomere properties and synchronicity of cell movement, detecting effects of drugs and of a gene deletion that affects cardiac contractility. Our approach contains a new method to measure sarcomere length from videos of labeled myofibrils and calculates single cell synchronicity as a novel functional assay. These innovative methods were combined with traction force microscopy and cross-correlation to deliver a new computational platform that characterizes the contractility of micropatterned hiPSC-CMs. The mechanical output of unpatterned hiPSC-CMs can also be quantified (Online Figure XI), except sarcomere length because we designed that method for cells with aligned myofibrils (Online Methods). Therefore, as long as attachment to a deformable substrate is stable and a more mature shape and alignment of myofibrils are observed, our approach can potentially analyze any type of single hiPSC-CM in these conditions. This platform has several advantages over earlier methods such as piezoelectric sensors,[36] atomic force microscopy[37], and micropipette aspiration[38]. Our approach is less invasive than previous single cell methods; importantly, it does not require skilled technical expertise for acquiring and analyzing data, broadening the accessibility and impact of these investigations. The integration of distinct video-based methods in the same computational platform facilitates the comparison of parameters and increases the versatility of functional analysis. This platform was developed for using after cell differentiation, fabrication of hydrogel substrates, micropatterning, fluorescent labeling of myofibrils and video acquisition (Online Figure I). The throughput of our platform can only be limited by low computational power of computers to be used. However, achieving a high throughput status will also require automation of cell differentiation, device fabrication, fluorescent labeling and microscopy. Our method is consistent with current increases in the use of cell micropatterning to model cardiac function with hiPSC-CMs[8, 9, 19, 39, 40] and provides the ability of researchers without a computational background to perform these assays.

We tested the ability of our video-based methods to quantify contractile changes in micropatterned hiPSC-CMs; specifically, we detected alterations in the mechanical output induced by caffeine, isoproterenol, and omecamtiv mecarbil. Adding caffeine increases the concentrations of cytosolic calcium.[41] Abruptly increasing the extracellular concentration of caffeine instantaneously halts the beating of hiPSC-CMs by depleting calcium stores in the sarcoplasmic reticulum.[42] Consistent with these reports, our data revealed an abrupt increase in mechanical output after the addition of caffeine, as well as a decrease in the kinetics of relaxation (Figure 2C). With isoproterenol, we validated the ability of our platform to detect changes in contractility under different drug concentrations and the use of omecamtiv mecarbil allowed us to demonstrate the need to detect acute and chronic effects for the same drug.

Isoproterenol is a beta-adrenergic agonist that affects biological mechanisms that alter CM contractility,[43] but the contractile effects of isoproterenol also depend on its extracellular concentration.[23, 24] The consistent increase in single cell mechanical output and beat rate

upon incubation in 0.1 μM demonstrated the ability of this system to detect the inotropic effects of isoproterenol (Figure 3 and Online Figure VI). However, the low magnitude of this increase and the drastic decrease in mechanical output after incubation in 1 μM also show that these cells do not fully recapitulate the contractile physiology of a well-matured myocardial tissue.

The same trend in the variation of contractile and kinetic parameters of mechanical output was obtained from analyzing the videos obtained through distinct imaging modalities (Figure 3). In addition, our sarcomere-mapping approach showed that a positive inotropic response was related to increased sarcomere shortening, while the average maximal length was maintained constant (Figure 5D). However, our approach revealed a difference in the magnitude of variation in mechanical output induced by 1 μM isoproterenol (Figure 3). Specifically, traction force microscopy showed a dramatic decrease in force and power outputs (Figure 3B,C) that was not identified from tracking the displacement of myofibrils (Figure 3E,F) or from cellular displacement on bright-field microscopy (Figure 3H,I). This difference suggests that variations in intracellular displacement do not directly relate to variations in force generation, even when reflecting the same general trend. In addition, traction force microscopy performed better than cross-correlation of bright-field videos (Online Figure VI) in detecting isoproterenol-induced contractile variations with statistical significance from a population of imaged cells. This observation suggests that our bright-field analysis tool can be improved in future studies, perhaps by segmenting cell features before analysis to eliminate potential image artifacts[44] or by using polarized light to better capture sarcomeres.[45] However, segmentation of cell area requires a clear intensity difference between the cell ROI and its exterior. A decrease in maximal sarcomere length and values of sarcomere shortening similar to baseline (no ISO) was observed for 1 μM, suggesting a decrease in intracellular tension at this concentration. To model cellular responses to high concentrations of isoproterenol, further research must address the mechanisms underpinning how mechanical output is regulated by sarcomere length under different isoproterenol concentrations.

Our analyses of the acute effects of omecamtiv mecarbil revealed by traction force microscopy and cross-correlation of bright-field videos also returned divergent results. Omecamtiv mecarbil had unexpected effects on cell contractility and in chronically damaging myofibrils (Figure 4C). The contractile effects of omecamtiv mecarbil in CMs have been previously reported to be atypical when compared with the effects of other inotropes.[23] Omecamtiv mecarbil acts specifically on cardiac myosin by increasing the time of its strong actin-bound state[25]; it also delays the relaxation of myofibris.[46] Consistent with this information, our data showed an increase in the time of contractions at higher drug concentrations (Online Figure VII D) and an increased *br* at lower drug concentration (Online Figure VII E). Omecamtiv mecarbil significantly shortened sarcomeres (Figure 5E–G), suggesting that the oscillatory contractions of sarcomeres and overlap between sarcomeres (Figure 4B and Online Movie IX) could result from increased intracellular tension. This possibility is supported by established relationships among calcium overload, tension, and the function of sarcomeres.[47] Future research is necessary to understand the effects of omecamtiv mecarbil in the function and organization of sarcomeres in relation to the mechanical output of micropatterned hiPSC-CMs. In addition, the chronic effects on

myofibril damage were unexpected and this observation should be further investigated taking into consideration mechanisms of sarcomere assembly and myogenic maturity.

We tested measuring the asynchronicity of beating of micropatterned hiPSC-CMs expressing decreased levels of MYBPC3. A decreased ability to generate contractile forces was previously identified in hiPSC-CMs expressing low levels of MYBPC3.[9] Importantly, we validated the use of parameters of asynchronicity in association with other parameters calculated from image analysis to potentially detect disease states involving contractile defects in micropatterned hiPSC-CMs.

As observed in Figure 3 and Figure 4, analyses of cell movement, estimations of force, and analyses of sarcomere movement may not yield curves with similar kinetics or magnitudes because they are derived from videos of different moving structures that have different mechanical properties. Bright-field videos contain information on the movement of the cell, which results from the propagation of sarcomere movement through a viscoelastic intracellular fluid environment that is different from the elastic polyacrylamide hydrogel and different from the physically interconnected sarcomeres in myofibrils. Therefore, the material mechanical properties of the different imaged milieus naturally affected their movement. The movement of microbeads in the substrate is a measure of how much force is the cell pulling on the substrate, which depends on the force generated by actin-myosin interactions, the intracellular balance of these forces, and the stability of extracellular adhesions. Although imaging myofibrils in live cells may be the closest we can come to evaluating actin-myosin interactions, this method does not provide information on the number of phosphorylated myosin heads and on the number of active myosins. In conclusion, cell movement, substrate movement, and myofibril movement are related, but do not necessarily reflect the same contractile properties of the cell because they involve the movement of materials with different material properties, highlighting the need for integrating data from distinct imaging modalities to well characterize cell mechanical output.

In summary, this platform quantifies critical parameters that evaluate the contractile performance of hiPSC-CMs. By considering how sarcomere and contractile movement relate to force generation, our unique approach provides a combination of methods for measuring contractile phenotypes.

Supplementary Material

Refer to Web version on PubMed Central for supplementary material.

Acknowledgments

We thank members of the Pruitt, Srivastava and Conklin laboratories. We thank Professor Ken Campbell for helpful discussions.

SOURCES OF FUNDING

This study was supported by American Heart Association Fellowship 14POST18360018, Canadian Institutes of Health Research postdoctoral fellowship 129844, the National Science Foundation (MIKS-1136790), and the

National Institutes of Health (R01-EB006745, R21-HL130993–01, and seed grants from Stanford CVI, BioX, and ChEM-H.

Nonstandard Abbreviations and Acronyms

CMs	cardiac myocytes
hiPSC-CMs	human induced pluripotent stem cell-derived cardiac myocytes
ROI	region of interest
d	mean displacement
d_{max}	maximal mean displacement
V	mean velocity
V_c	peak velocity of contraction
V_R	peak velocity of relaxation
F	magnitude of force vector
ΣF	sum of magnitudes of force vectors
ΣF_{max}	maximal sum of magnitudes of force vectors
P	power
P_c	peak power of contraction
P_R	peak power of relaxation
br	beat rate
$\hat{t}$	time between contraction and relaxation peaks
sl	sarcomere length
ss	sarcomere shortening
MYBPC3	myosin binding protein C3
a_θ	spatial asynchronicity
a_δ	temporal asynchronicity
ISO	isoproterenol
OM	omecamtiv mecarbil

References

1. Brady AJ. Mechanical properties of isolated cardiac myocytes. Physiol Rev. 1991; 71:413–428. DOI: 10.1016/S0008-6363(98)00019-4 [PubMed: 2006219]

2. Nadal-Ginard B, Mahdavi V. Molecular basis of cardiac performance. Plasticity of the myocardium generated through protein isoform switches. J Clin Invest. 1989; 84:1693–1700. DOI: 10.1172/JCI114351 [PubMed: 2687327]
3. Talkhabi M, Aghdami N, Baharvand H. Human cardiac myocyte generation from pluripotent stem cells: A state-of-art. Life sciences. 2016; 145:98–113. [PubMed: 26682938]
4. Yang X, Pabon L, Murry CE. Engineering adolescence: Maturation of human pluripotent stem cell-derived cardiac myocytes. Circ Res. 2014; 114:511–523. DOI: 10.1161/CIRCRESAHA.114.300558 [PubMed: 24481842]
5. Wang G, McCain ML, Yang L, He A, Pasqualini FS, Agarwal A, Yuan H, Jiang D, Zhang D, Zangi L, Geva J, Roberts AE, Ma Q, Ding J, Chen J, Wang DZ, Li K, Wang J, Wanders RJ, Kulik W, Vaz FM, Laflamme MA, Murry CE, Chien KR, Kelley RI, Church GM, Parker KK, Pu WT. Modeling the mitochondrial cardiomyopathy of barth syndrome with induced pluripotent stem cell and heart-on-chip technologies. Nat Med. 2014; 20:616–623. DOI: 10.1038/nm.3545 [PubMed: 24813252]
6. Ribeiro MC, Tertoolen LG, Guadix JA, Bellin M, Kosmidis G, D'Aniello C, Monshouwer-Kloots J, Goumans MJ, Wang YL, Feinberg AW, Mummery CL, Passier R. Functional maturation of human pluripotent stem cell derived cardiac myocytes in vitro–correlation between contraction force and electrophysiology. Biomaterials. 2015; 51:138–150. DOI: 10.1016/j.biomaterials.2015.01.067 [PubMed: 25771005]
7. Ribeiro AJ, Ang YS, Fu JD, Rivas RN, Mohamed TM, Higgs GC, Srivastava D, Pruitt BL. Contractility of single cardiac myocytes differentiated from pluripotent stem cells depends on physiological shape and substrate stiffness. Proc Natl Acad Sci U S A. 2015; 112:12705–12710. DOI: 10.1073/pnas.1508073112 [PubMed: 26417073]
8. Kijlstra JD, Hu D, Mittal N, Kausel E, van der Meer P, Garakani A, Domian IJ. Integrated analysis of contractile kinetics, force generation, and electrical activity in single human stem cell-derived cardiac myocytes. Stem Cell Reports. 2015; 5:1226–1238. DOI: 10.1016/j.stemcr.2015.10.017 [PubMed: 26626178]
9. Birket MJ, Ribeiro MC, Kosmidis G, Ward D, Leitoguinho AR, van de Pol V, Dambrot C, Devalla HD, Davis RP, Mastroberardino PG, Atsma DE, Passier R, Mummery CL. Contractile defect caused by mutation in mybpc3 revealed under conditions optimized for human psc-cardiac myocyte function. Cell Rep. 2015; 13:733–745. DOI: 10.1016/j.celrep.2015.09.025 [PubMed: 26489474]
10. Ang YS, Rivas RN, Ribeiro AJ, Srivas R, Rivera J, Stone NR, Pratt K, Mohamed TM, Fu JD, Spencer CI, Tippens ND, Li M, Narasimha A, Radzinsky E, Moon-Grady AJ, Yu H, Pruitt BL, Snyder MP, Srivastava D. Disease model of gata4 mutation reveals transcription factor cooperativity in human cardiogenesis. Cell. 2016; 167:1734–1749.e1722. DOI: 10.1016/j.cell.2016.11.033 [PubMed: 27984724]
11. Lan F, Lee AS, Liang P, Sanchez-Freire V, Nguyen PK, Wang L, Han L, Yen M, Wang Y, Sun N, Abilez OJ, Hu S, Ebert AD, Navarrete EG, Simmons CS, Wheeler M, Pruitt B, Lewis R, Yamaguchi Y, Ashley EA, Bers DM, Robbins RC, Longaker MT, Wu JC. Abnormal calcium handling properties underlie familial hypertrophic cardiomyopathy pathology in patient-specific induced pluripotent stem cells. Cell Stem Cell. 2013; 12:101–113. DOI: 10.1016/j.stem.2012.10.010 [PubMed: 23290139]
12. Huebsch N, Loskill P, Deveshwar N, Spencer CI, Judge LM, Mandegar MA, C BF, Mohamed TM, Ma Z, Mathur A, Sheehan AM, Truong A, Saxton M, Yoo J, Srivastava D, Desai TA, So PL, Healy KE, Conklin BR. Miniaturized ips-cell-derived cardiac muscles for physiologically relevant drug response analyses. Sci Rep. 2016; 6:24726.doi: 10.1038/srep24726 [PubMed: 27095412]
13. Feaster TK, Cadar AG, Wang L, Williams CH, Chun YW, Hempel JE, Bloodworth N, Merryman WD, Lim CC, Wu JC, Knollmann BC, Hong CC. Matrigel mattress: A method for the generation of single contracting human-induced pluripotent stem cell-derived cardiac myocytes. Circ Res. 2015; 117:995–1000. DOI: 10.1161/CIRCRESAHA [PubMed: 26429802]
14. Beussman KM, Rodriguez ML, Leonard A, Taparia N, Thompson CR, Sniadecki NJ. Micropost arrays for measuring stem cell-derived cardiac myocyte contractility. Methods. 2016; 94:43–50. DOI: 10.1016/j.ymeth.2015.09.005 [PubMed: 26344757]
15. van Meer BJ, Tertoolen LG, Mummery CL. Concise review: Measuring physiological responses of human pluripotent stem cell derived cardiac myocytes to drugs and disease. Stem Cells. 2016; 34:2008–2015. DOI: 10.1002/stem.2403 [PubMed: 27250776]

16. Zhu R, Blazeski A, Poon E, Costa KD, Tung L, Boheler KR. Physical developmental cues for the maturation of human pluripotent stem cell-derived cardiac myocytes. Stem Cell Res Ther. 2014; 5:117.doi: 10.1186/scrt507 [PubMed: 25688759]

17. Ips cells 10 years later. Cell. 2016; 166:1356–1359. DOI: 10.1016/j.cell.2016.08.043 [PubMed: 27610558]

18. Aoi T. 10th anniversary of ips cells: The challenges that lie ahead. J Biochem. 2016; 160:121–129. DOI: 10.1093/jb/mvw044 [PubMed: 27387749]

19. Del Alamo JC, Lemons D, Serrano R, Savchenko A, Cerignoli F, Bodmer R, Mercola M. High throughput physiological screening of ipsc-derived cardiac myocytes for drug development. Biochim Biophys Acta. 2016; 1863:1717–1727. DOI: 10.1016/j.bbamcr.2016.03.003 [PubMed: 26952934]

20. Blaber J, Adair B, Antoniou A. Ncorr: Open-source 2d digital image correlation matlab software. Exp Mech. 2015; 55:1105–1122. DOI: 10.1007/s11340-015-0009-1

21. Thielicke W, Stamhuis EJ. PIVlab - Towards user-friendly, affordable and accurate digital particle image velocimetry in MATLAB. J Open Res Software. 2(1):e30. doi: http://dx.doi.org/10.5334/jors.bl.

22. Tseng Q, Duchemin-Pelletier E, Deshiere A, Balland M, Guillou H, Filhol O, Thery M. Spatial organization of the extracellular matrix regulates cell-cell junction positioning. Proc Natl Acad Sci U S A. 2012; 109:1506–1511. DOI: 10.1073/pnas.1106377109 [PubMed: 22307605]

23. Butler L, Cros C, Oldman KL, Harmer AR, Pointon A, Pollard CE, Abi-Gerges N. Enhanced characterization of contractility in cardiac myocytes during early drug safety assessment. Toxicol Sci. 2015; 145:396–406. DOI: 10.1093/toxsci/kfv062 [PubMed: 25820236]

24. Katano Y, Endoh M. Effects of a cardiotonic quinolinone derivative y-20487 on the isoproterenol-induced positive inotropic action and cyclic amp accumulation in rat ventricular myocardium: Comparison with rolipram, ro 20–1724, milrinone, and isobutylmethylxanthine. J Cardiovasc Pharmacol. 1992; 20:715–722. DOI: 10.1097/00005344-199211000-00005 [PubMed: 1280732]

25. Liu LC, Dorhout B, van der Meer P, Teerlink JR, Voors AA. Omecamtiv mecarbil: A new cardiac myosin activator for the treatment of heart failure. Expert Opin Investig Drugs. 2016; 25:117–127. DOI: 10.1517/13543784.2016.1123248

26. Gulick T, Pieper SJ, Murphy MA, Lange LG, Schreiner GF. A new method for assessment of cultured cardiac myocyte contractility detects immune factor-mediated inhibition of beta-adrenergic responses. Circulation. 1991; 84:313–321. doi: http://dx.doi.org/10.1161/01.CIR.84.1.313. [PubMed: 1647897]

27. Decker ML, Behnke-Barclay M, Cook MG, Lesch M, Decker RS. Morphometric evaluation of the contractile apparatus in primary cultures of rabbit cardiac myocytes. Circ Res. 1991; 69:86–94. doi: http://dx.doi.org/10.1161/01.RES.69.1.86. [PubMed: 2054944]

28. Forough R, Scarcello C, Perkins M. Cardiac biomarkers: A focus on cardiac regeneration. J Tehran Heart Cent. 2011; 6:179–186. [PubMed: 23074366]

29. Ibrahim M, Gorelik J, Yacoub MH, Terracciano CM. The structure and function of cardiac t-tubules in health and disease. Proc Biol Sci. 2011; 278:2714–2723. DOI: 10.1098/rspb.2011.0624 [PubMed: 21697171]

30. Tsai MS, Tang W, Sun S, Wang H, Freeman G, Chen WJ, Weil MH. Individual effect of components of defibrillation waveform on the contractile function and intracellular calcium dynamics of cardiac myocytes. Crit Care Med. 2009; 37:2394–2401. DOI: 10.1097/CCM.0b013e3181a02ea1 [PubMed: 19531953]

31. Roman-Campos D, Sales-Junior P, Duarte HL, Gomes ER, Lara A, Campos P, Rocha NN, Resende RR, Ferreira A, Guatimosim S, Gazzinelli RT, Ropert C, Cruz JS. Novel insights into the development of chagasic cardiomyopathy: Role of pi3kinase/no axis. Int J Cardiol. 2013; 167:3011–3020. DOI: 10.1016/j.ijcard.2012.09.020 [PubMed: 23031286]

32. Wigle ED, Rakowski H, Kimball BP, Williams WG. Hypertrophic cardiomyopathy. Clinical spectrum and treatment. Circulation. 1995; 92:1680–1692. doi: http://dx.doi.org/10.1161/01.CIR.92.7.1680. [PubMed: 7671349]

33. Fineschi V, Silver MD, Karch SB, Parolini M, Turillazzi E, Pomara C, Baroldi G. Myocardial disarray: An architectural disorganization linked with adrenergic stress? Int J Cardiol. 2005; 99:277–282. DOI: 10.1016/j.ijcard.2004.01.022 [PubMed: 15749187]
34. Harris SP, Bartley CR, Hacker TA, McDonald KS, Douglas PS, Greaser ML, Powers PA, Moss RL. Hypertrophic cardiomyopathy in cardiac myosin binding protein-c knockout mice. Circ Res. 2002; 90:594–601. doi: http://dx.doi.org/10.1161/01.RES.0000012222.70819.64. [PubMed: 11909824]
35. Carrier L, Knoll R, Vignier N, Keller DI, Bausero P, Prudhon B, Isnard R, Ambroisine ML, Fiszman M, Ross J Jr, Schwartz K, Chien KR. Asymmetric septal hypertrophy in heterozygous cmybp-c null mice. Cardiovasc Res. 2004; 63:293–304. DOI: 10.1016/j.cardiores.2004.04.009 [PubMed: 15249187]
36. Iribe G, Helmes M, Kohl P. Force-length relations in isolated intact cardiac myocytes subjected to dynamic changes in mechanical load. Am J Physiol Heart Circ Physiol. 2007; 292:H1487–1497. DOI: 10.1152/ajpheart.00909.2006 [PubMed: 17098830]
37. Domke J, Parak WJ, George M, Gaub HE, Radmacher M. Mapping the mechanical pulse of single cardiac myocytes with the atomic force microscope. Eur Biophys J. 1999; 28:179–186. DOI: 10.1007/s002490050198 [PubMed: 10192933]
38. Sweitzer NK, Moss RL. Determinants of loaded shortening velocity in single cardiac myocytes permeabilized with alpha-hemolysin. Circ Res. 1993; 73:1150–1162. DOI: 10.1161/01.RES.73.6.1150 [PubMed: 8222086]
39. Denning C, Borgdorff V, Crutchley J, Firth KS, George V, Kalra S, Kondrashov A, Hoang MD, Mosqueira D, Patel A, Prodanov L, Rajamohan D, Skarnes WC, Smith JG, Young LE. Cardiac myocytes from human pluripotent stem cells: From laboratory curiosity to industrial biomedical platform. Biochim Biophys Acta. 2016; 1863:1728–1748. DOI: 10.1016/j.bbamcr.2015.10.014 [PubMed: 26524115]
40. Napiwocki, BN., Salick, MR., Ashton, RS., Crone, WC. Controlling hESC-CM cell morphology on patterned substrates over a range of stiffness. In: Korach, SC.Tekalur, AS., Zavattieri, P., editors. Mechanics of biological systems and materials, Volume 6: Proceedings of the 2016 annual conference on experimental and applied mechanics. Vol. 2017. Cham: Springer International Publishing; p. 161-168.
41. O'Neill SC, Eisner DA. A mechanism for the effects of caffeine on ca2+ release during diastole and systole in isolated rat ventricular myocytes. J Physiol. 1990; 430:519–536. DOI: 10.1113/jphysiol.1990.sp018305 [PubMed: 2086772]
42. Itzhaki I, Rapoport S, Huber I, Mizrahi I, Zwi-Dantsis L, Arbel G, Schiller J, Gepstein L. Calcium handling in human induced pluripotent stem cell derived cardiac myocytes. PLoS ONE. 2011; 6doi: 10.1371/journal.pone.0018037
43. Wallukat G. The beta-adrenergic receptors. Herz. 2002; 27:683–690. DOI: 10.1007/s00059-002-2434-z [PubMed: 12439640]
44. Yin Z, Li K, Kanade T, Chen M. Understanding the optics to aid microscopy image segmentation. Med Image Comput Comput Assist Interv. 2010; 13:209–217. DOI: 10.1007/978-3-642-15705-9_26
45. Aronson JF. Polarized light observations on striated muscle contraction in a mite. J Cell Biol. 1967; 32:169–179. [PubMed: 10976208]
46. Nagy L, Kovacs A, Bodi B, Pasztor ET, Fulop GA, Toth A, Edes I, Papp Z. The novel cardiac myosin activator omecamtiv mecarbil increases the calcium sensitivity of force production in isolated cardiac myocytes and skeletal muscle fibres of the rat. Br J Pharmacol. 2015; Epub ahead of print. doi: 10.1111/bph.13235
47. Davis J, Davis LC, Correll RN, Makarewich CA, Schwanekamp JA, Moussavi-Harami F, Wang D, York AJ, Wu H, Houser SR, Seidman CE, Seidman JG, Regnier M, Metzger JM, Wu JC, Molkentin JD. A tension-based model distinguishes hypertrophic versus dilated cardiomyopathy. Cell. 2016; 165:1147–1159. DOI: 10.1016/j.cell.2016.04.002 [PubMed: 27114035]

NOVELTY AND SIGNIFICANCE

What Is Known?

- Human induced pluripotent stem cells (hiPSCs) can be differentiated into cardiac myocytes (hiPSC-CMs) and model human heart function.
- Fetal-like disorganization of the sarcomere-based contractile machinery in hiPSC-CMs limits their use as models of cardiac contractility.
- Culturing single hiPSC-CMs on rectangular protein micropatterns on hydrogels improves their contractility due to enhanced organization of sarcomeres.

What New Information Does This Article Contribute?

- A new platform was developed to assay the contractile performance of single micropatterned hiPSC-CMs from videos acquired with live-cell imaging.
- Parameters of cell beating are derived from videos, as well as sarcomere shortening and the level of synchronicity of beating within a cell.
- Our method can detect contractile variations induced by drugs and disease states in a minimally invasive and non-destructive manner.

Measuring the contractile performance of single cardiac myocytes (CMs) can assay the effects of drugs, diseases or pharmacological interventions in the function of the heart. We developed a novel platform for measuring the contractile performance of CMs differentiated from human induced pluripotent stem cells (hiPSC-CMs). Assaying these cells has high potential for predicting drug effects and modeling diseases. We specifically designed our platform for assaying rectangular single hiPSC-CMs attached to soft hydrogels because the intracellular organization of the sarcomere-based contractile machinery is improved in these conditions, which further improves their contractility. Our approach integrates different image-based analytical tools to calculate contractile and kinetic parameters of beating. These tools analyze videos of beating cells acquired with brightfield microscopy and fluorescence videos of labeled sarcomeres and labeled particles in the moving hydrogel under the cell. We integrated these different video analyses to comprehensively quantify and evaluate different properties of hiPSC-CM contractility: cell movement, mechanical output and sarcomere activity. Overall, we validated the ability of our approach to detect contractile variations or defects in hiPSC-CMs induced by drugs or changes in sarcomere proteins. This platform is now available for anyone in need of comprehensively assaying hiPSC-CM contractility to study mechanisms that regulate cardiac function.

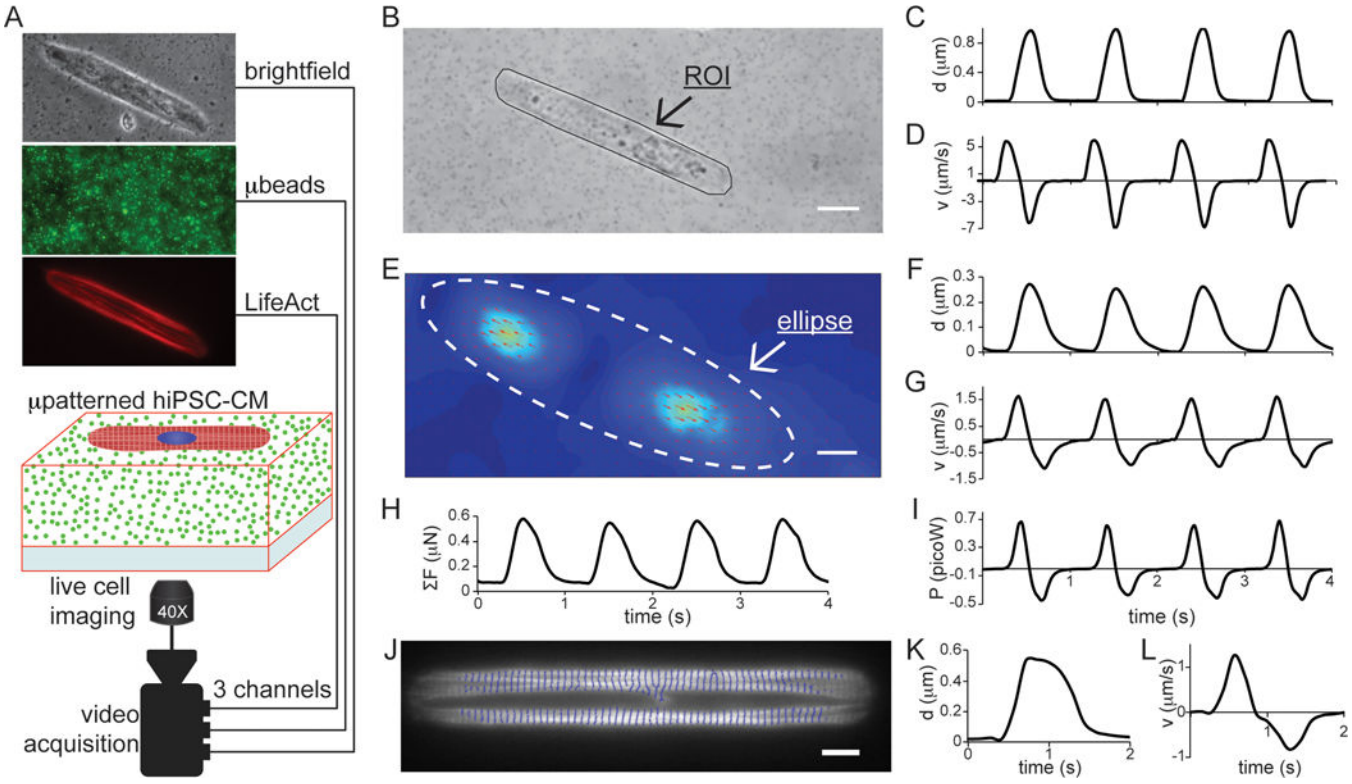

Figure 1. Registering the contractile mechanical output of micropatterned hiPSC-CMs from microscopy videos

A, Three classes of videos of beating micropatterned hiPSC-CMs were acquired with microscopy: bright-field videos, videos of fluorescent microbeads embedded in the deformable gel substrate, and videos of moving fluorescent myofibrils. **B**, A region of interest (ROI) was defined around the contour of the cell; movement within this region was analyzed with cross-correlation from bright-field videos. Scale bar: 15 μm. **C**, Cell average displacement (*d*) due to the contractile activity of beating within the ROI was quantified and plotted as a function of time, yielding a *d*-curve. **D**, Average velocity of displacement (*V*) within the ROI was calculated from the first derivative of displacement and plotted as a function of time, yielding a *V*-curve. **E**, Average displacement (*d*) of microbeads embedded in the gel substrate was also quantified with cross-correlation from fluorescent videos. An ellipse calculated from the dimension of the ROI was automatically drawn to limit the calculation of displacement to this region. Scale bar: 15 μm. **F**, *d*-curve of microbeads plotted as a function of time. **G**, *V*-curve of microbeads plotted as a function of time. **H**, Contractile force (Σ*F*) estimated with traction force microscopy from the displacement map of microbeads (E) and plotted as a function of time, yielding an F-curve. **I**, Power (*P*) was calculated by multiplying Σ*F* by *V* of microbeads and plotted as a function of time, yielding a *P*-curve. **J**, The regions occupied by sarcomeres within labeled myofibrils were skeletonized. This cell is not the cell shown in B. **K**, *d*-curve of myofibrils of cell in J. **L**, myofibril *V*-curve for cell in J. Scale bar: 10 μm.

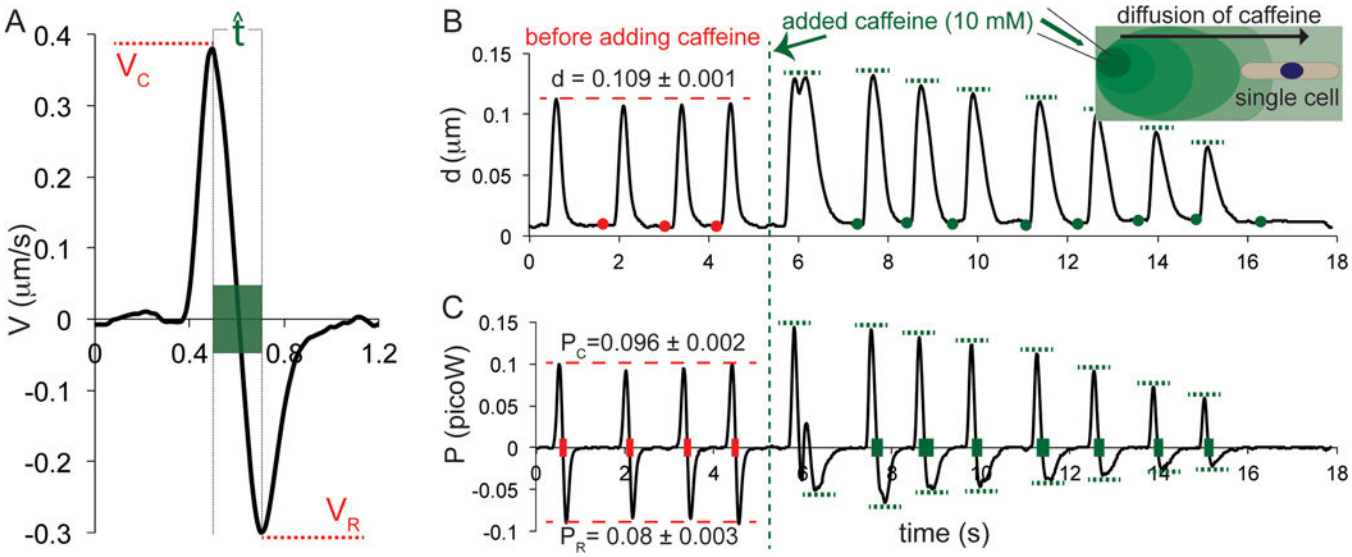

Figure 2. Parameters of contractile cycles are derived from plots

A, We determined three kinetic parameters from *V*-curves that represent each contractile cycle: V_C is the peak velocity of contraction, V_R is the peak velocity of relaxation, and $\hat{t}$ (green rectangle) is the time between the peak velocity of contraction and the peak velocity of relaxation. The *V*-curve was calculated from the displacement (*d*) of microbeads. **B**, Variations in the *d*-curve derived from videos of moving microbeads were analyzed after slowly increasing the concentration of caffeine in the extracellular milieu. We determined maximum values (dashed lines) and minimum values (circles) of d. **C**, *P* was also analyzed while increasing the concentration of caffeine. *P* was calculated by multiplying F by *V* to determine the peak power of contraction (P_C; upper dashed lines), the peak power of relaxation (P_R; lower dashed lines), and $\hat{t}$ (rectangles).

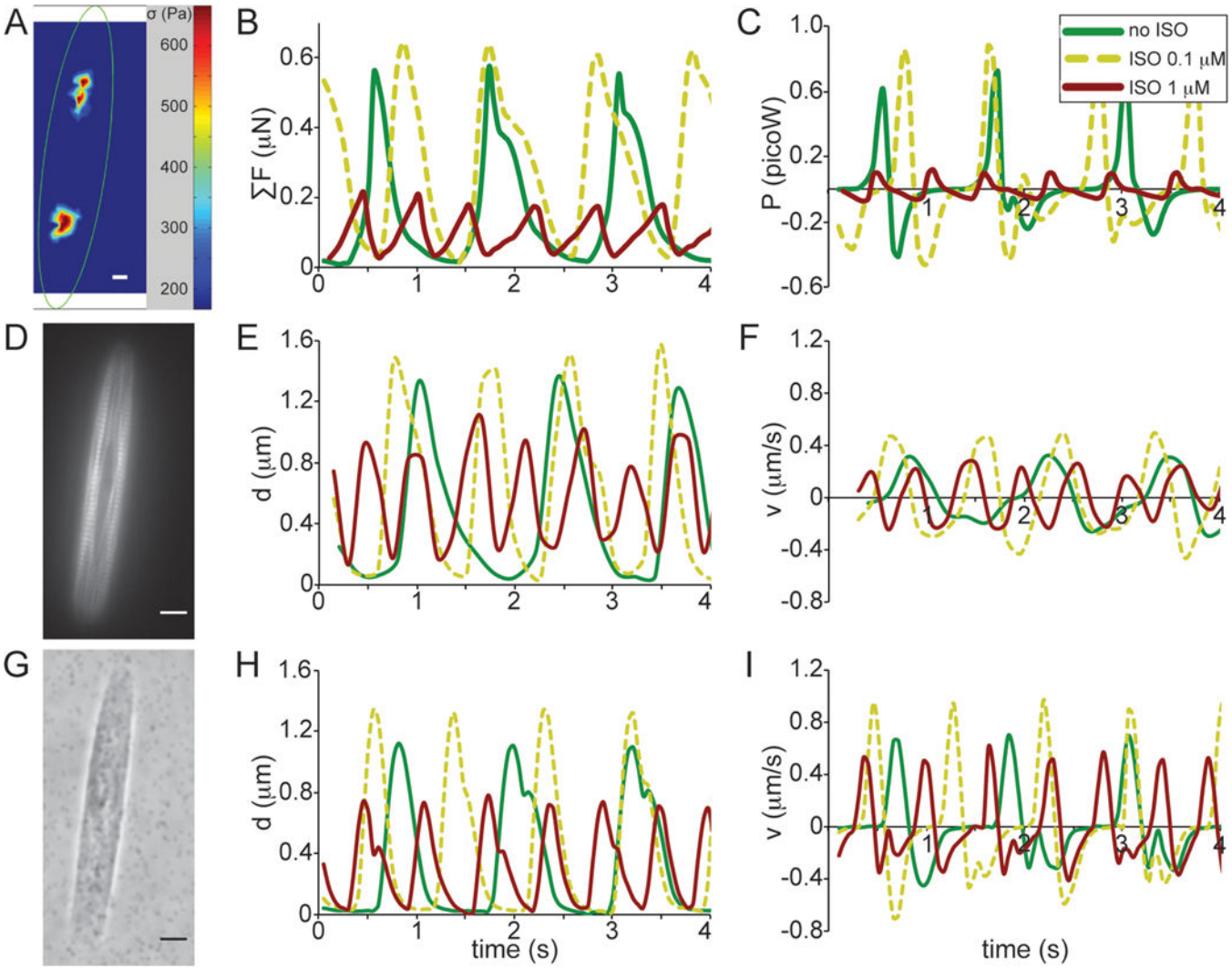

Figure 3. Detection of isoproterenol (ISO)-induced variations in the mechanical output of a single micropatterned hiPSC-CM

We used two different concentrations of isoproterenol (0.1 μM and 1 μM) to test the ability of our image analysis platform to detect contractile variations. **A**, Heat map in which cell-generated traction stresses on the surface of the gel substrate were estimated with traction force microscopy; *F* was calculated within the region delimited by an ellipse around the cell. **D**, Myofibrils were fluorescently labeled in the analyzed micropatterned hiPSC-CM (Online Movie V) and imaged for quantification of myofibril movement. **B**, *F*-curves and **C**, *P*-curves were estimated from videos of moving microbeads acquired before and after the cell was exposed to isoproterenol. **D**, Myofibrils were fluorescently labeled in the micropatterned hiPSC-CM (Online Movie V) and imaged to quantify myofibril movement. **E**, *d*-curves and **F**, *V*-curves calculated from videos of moving myofibrils before and after adding isoproterenol. **G**, Bright-field video of the analyzed single cell. **H**, *d*-curves and **I**, *V*-curves obtained from brighfield videos of the cell at different isoproterenol concentrations. Scale bar: 10 μm.

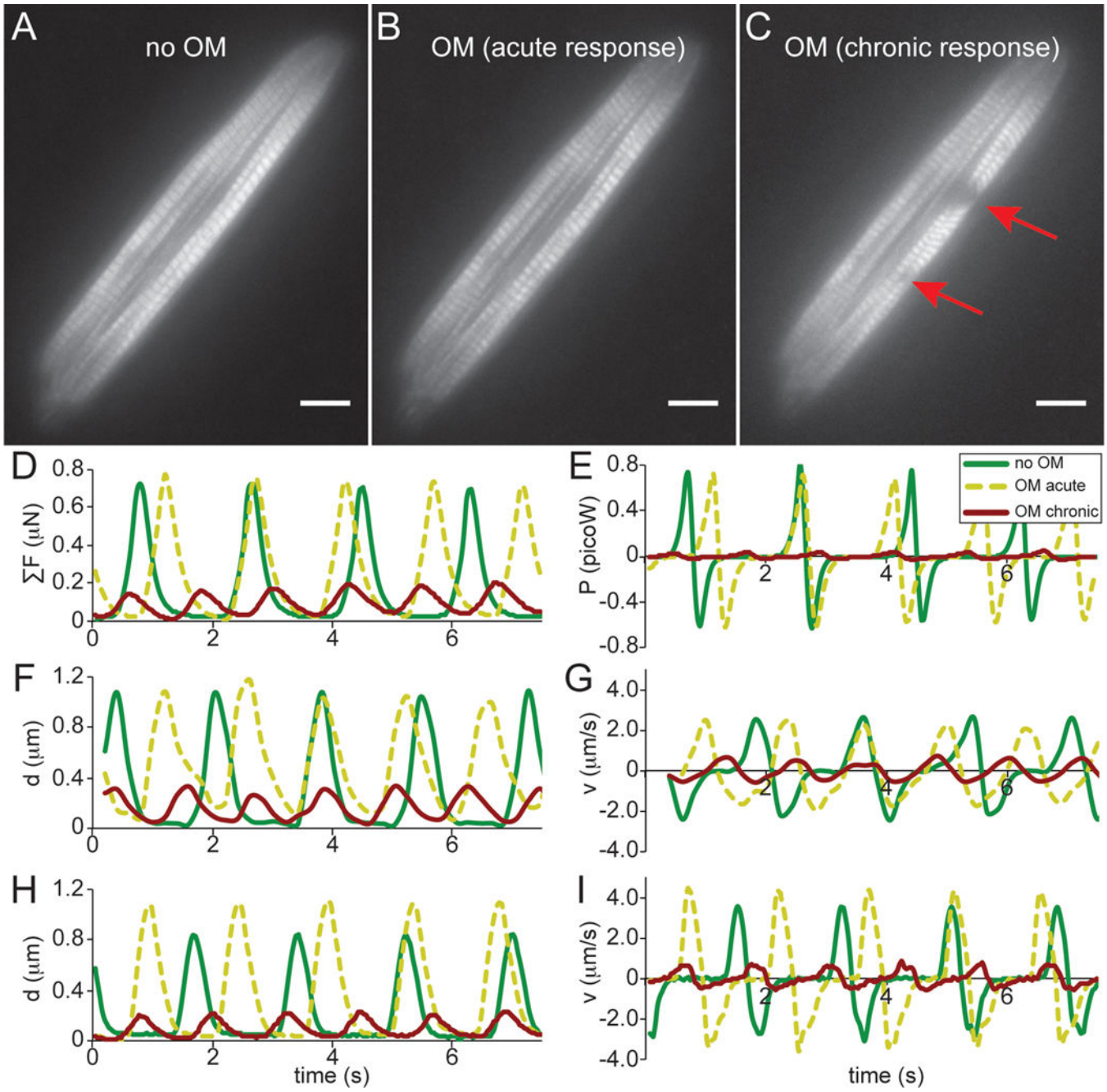

Figure 4. Validating the ability of our integrated platform to detect changes in the mechanical output of a single hiPSC-CM induced by omecamtiv mecarbil (OM)

OM was added to the extracellular milieu of a beating micropatterned hiPSC-CM at a concentration of 0.1 μM, and we acquired videos of microbeads in the substrate, of moving myofibrils, and of the cell before and after adding OM. **A**, Fluorescently labeled myofibrils before adding OM (Online Movie VIII). **B**, Acute tightening of sarcomeres detected within 10 s after adding OM (Online Movie IX). **C**, Chronic damage of myofibrils imaged 2 minutes after adding OM (Online Movie X). Red arrows point at the locations of myofibril damages. **D**, F-curves and **E**, *P*-curves were estimated from videos of moving microbeads

acquired before adding OM and after acute and chronic exposure. **F**, *d*-curves and **G**, *V*-curves calculated from videos of moving myofibrils. **H**, *d*-curves and **I**, *V*-curves obtained from brighfield videos of the cell. Scale bar: 10 μm.

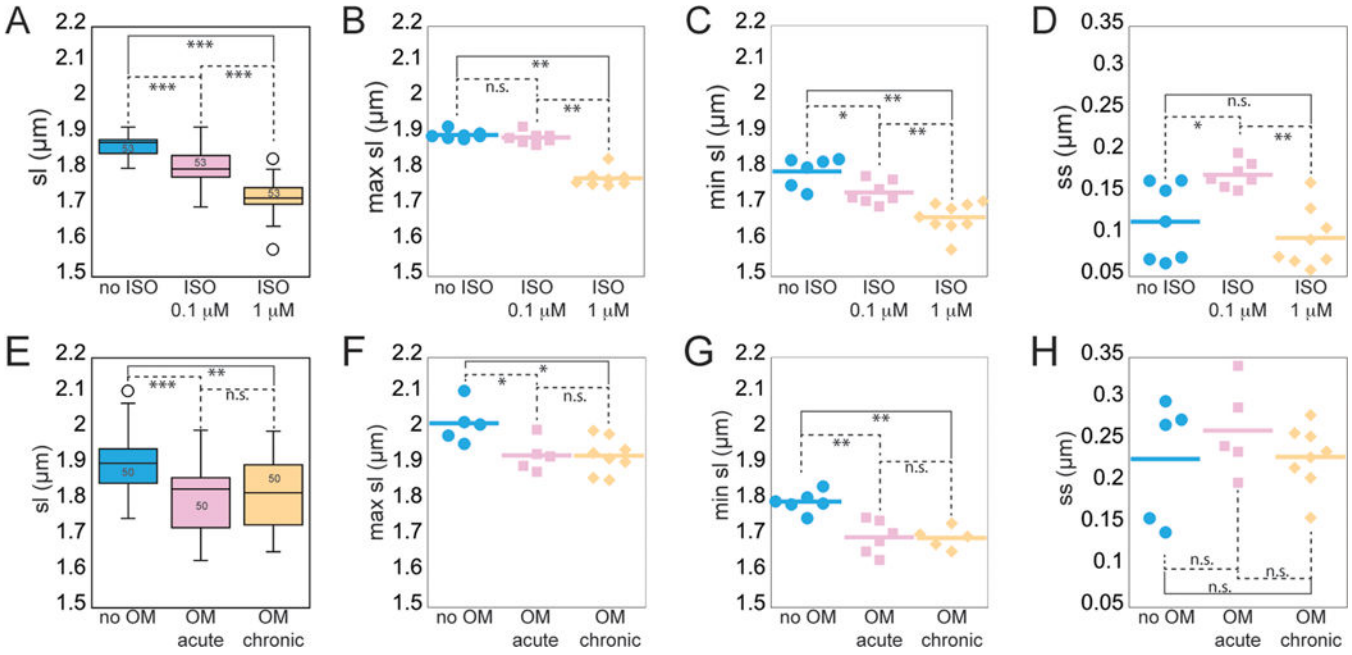

Figure 5. Detection of changes in sarcomere length and sarcomere shortening induced by isoproterenol (ISO) and omecamtiv mecarbil (OM)

We measured sarcomere length (sl) and sarcomere shortening (ss) from videos of myofibrils labeled in the beating micropatterned hiPSC-CMs in Figure 4 and Figure 6. **A and E**, Box plots of average sarcomere length values calculated for all frames of the analyzed videos (n=53 frames for the cell exposed to ISO (Online Movies V–VII); n=50 frames for the cell exposed to OM (Online Movies VIII–X). **B and F**, Maximum values of sarcomere length. **C and G**, minimum values of sarcomere length. **D and H**, sarcomere shortening calculated by subtracting the minimum values of sarcomere length from the maximum values of sarcomere length. Each point represents a value in the contractile curve of moving sarcomeres. *P<0.05, **P<0.01, and ***P<0.005 by the unpaired Wilcoxon-Mann-Whitney rank-sum test and by Bonferroni's all-pairs comparison test; n.s., not significant with any test. ANOVA P<0.001 (A–E) and ANOVA P<0.02 (F and G).

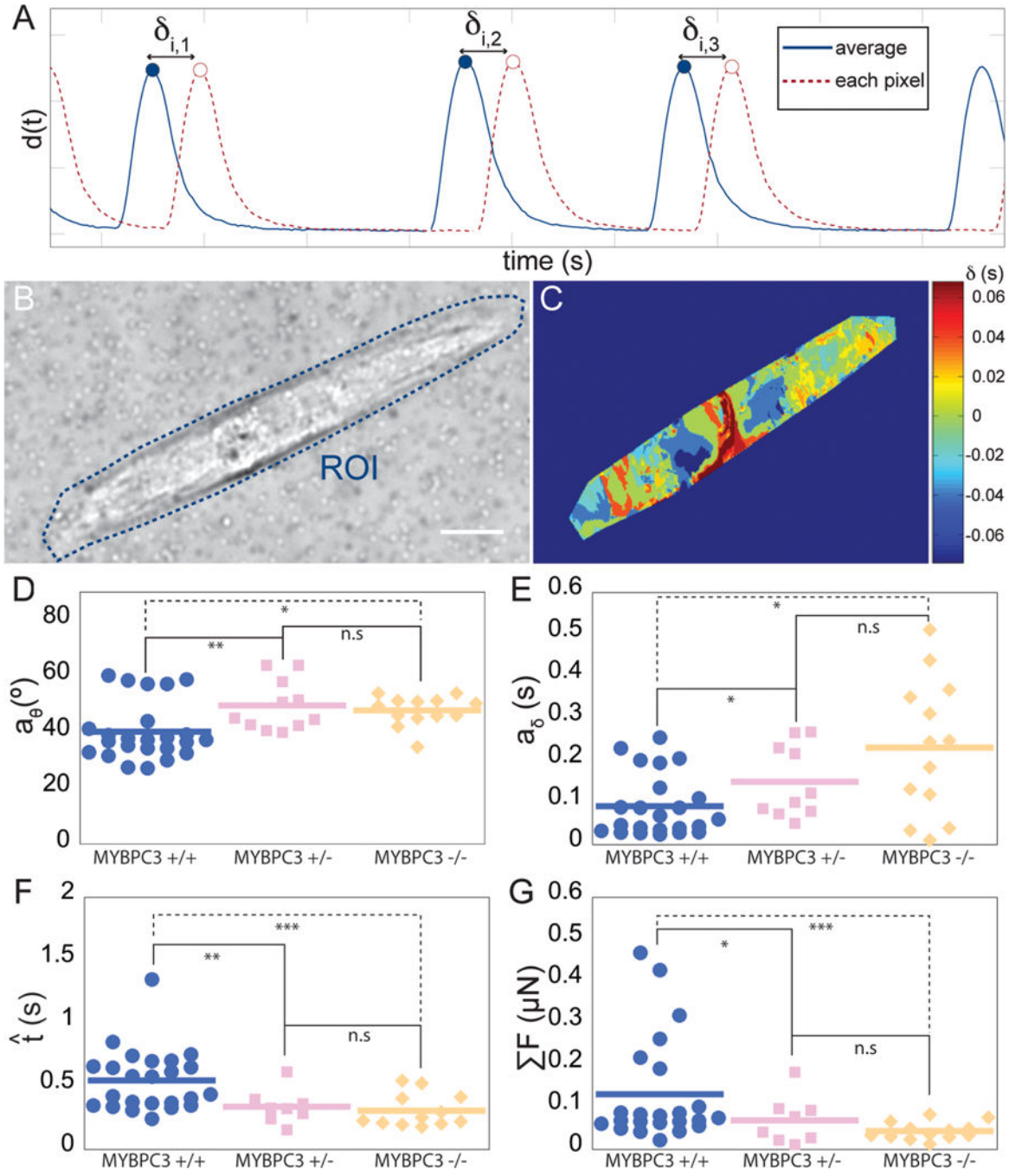

Figure 6. Measuring parameters of spatial (a_θ) or temporal (a_δ) asynchronicity in micropatterned hiPSC-CMs harboring homozygous and heterozygous knockout of the gene encoding MYBPC3

a_δ was calculated from the offset times (δ) of intracellular displacement. **A**, δ was determined for each pixel i within an ROI delimited by the borders of the cell by subtracting the time of each displacement peak for each pixel i by the time of the displacement peak for the average of displacement in the ROI. **B**, Representative ROI in a bright-field video of a beating micropatterned hiPSC-CM. **C**, Heat map of δ within the pixels of the ROI. **D-G**, parameters calculated from micropatterned hiPSC-CMs that lack both copies of the gene

encoding MYBPC3 (−/−) or that lack one copy of the gene (+/−). MYBPC3 +/+ cells contain both copies of the gene. **D**, a_θ. **E**, a_δ. **F**, $\hat{t}$. *P < 0.05, **P<0.01, and ***P<0.005 by the unpaired Wilcoxon-Mann-Whitney rank-sum test and by Bonferroni's all-pairs comparison test; n.s., not significant with any test. ANOVA P<0.01 (D–F) and ANOVA P<0.04 (G). Scale bar: 15 μm.